Intensity-Dependent Reflectance and Transmittance of Semiconductor Periodic Structures

Lukasz Brzozowski, Vladimir Sukhovatkin, Edward (Ted) H. Sargent, Anthony (Tony) J. SpringThorpe, and Marcius Extavour

***Abstract*—The intensity-dependent response of nonlinear Bragg-periodic epitaxially-grown InGaAs–InAlGaAs-based optical elements is reported over a broad spectral range 1.3–1.6 μm. Large changes in the transmittance and reflectance are observed as a function of incident power. Over most of this spectral region, the nonlinear response is dominated by the saturation of absorption. In the vicinity of 1.5 μm, the optical elements exhibit fluence-dependent Bragg diffraction. For low incident powers, the indices of refraction of structures are uniform and no coherent scattering takes place. With increased incident power a Bragg grating appears, resulting in the emergence of a fluence-dependent stopband in the transmittance and reflectance spectra.**

***Index Terms*—All-optical elements, Kerr nonlinearity, nonlinear optics, nonlinear-periodic structures, saturation of absorption, semiconductor multi-quantum-wells.**

I. Introduction

OPTICAL switching and pulse shaping would reduce optical-electrical-optical conversion and increase transparency in optical networks. A number of all-optical devices and elements have been proposed and fabricated for this purpose [1], [2].

Nonlinear Bragg-periodic structures offer a particularly wide variety of optical signal processing functions. These structures have been theoretically predicted and experimentally demonstrated to give rise to all-optical switching [3], [4], pulse compression [5]–[7], limiting [3], [8], [9], and logic operations [10]. In addition, nonlinear periodic structures support solitary waves—pulses that propagate without changing their shapes [11], [12].

A variety of interesting and promising approaches for combining third-order nonlinearity and Bragg periodicity has been proposed. Colloidal crystals provide a three-dimensional periodic framework into which materials exhibiting thermal [8], [13], and ultrafast nonlinearities [14] may be embedded. Fiber Bragg gratings [5], [7] and corrugated integrated optical waveguides [15] yield one-dimensional nonlinear periodic structures.

Manuscript received November 21, 2002; revised March 5, 2003. This work was supported by Nortel Networks and by the Natural Sciences and Engineering Research Council of Canada.

L. Brzozowski, V. Sukhovatkin, and E. H. Sargent are with the Department of Electrical and Computer Engineering, University of Toronto, Toronto, ON M5S 1A4, Canada.

A. J. SpringThorpe was with Nortel Networks, Nepean, ON K1Y 4H7, Canada. He is now with the Institute for Microstructural Sciences, National Research Council of Canada, Ottawa, ON, Canada.

M. Extavour was with Nortel Networks, Nepean, ON K1Y 4H7, Canada. He is now with the Department of Electrical and Computer Engineering, University of Toronto, Toronto, ON M5S 1A4, Canada.

Digital Object Identifier 10.1109/JQE.2003.813195

The optical elements analyzed in this work were grown using molecular beam epitaxy. They have a low initial refractive index contrast. This has been predicted to be a desirable condition for all-optical limiting and stable switching [3], [6], [9]. In addition, the optical elements were designed in such a way that there is a spectral overlap of the Bragg resonance with strongly nonlinear absorption edge of at least one constituent material [16], [17]. Recently, strong saturation of absorption and nonlinear index changes as large as $\Delta n = -0.14$ have been recorded in the bandedge region of $In_{0.530}Al_{0.141}Ga_{0.329}As$–$In_{0.530}Ga_{0.470}As$ multi-quantum-wells (MQWs) [18].

In the present work, nonlinear transmission and reflection measurements from these nonlinear Bragg periodic structures are reported over a wide spectral range relevant to telecommunication. Large changes in transmittance and reflectance are observed. Comparison is made between the intensity dependence of the response of:

- optical periodic elements that upon excitation with intense light exhibit Bragg contradirectional coupling;
- MQWs of a similar thickness and composition.

Nonlinear Bragg diffraction has opposite effects on the change in transmittance and on the change in reflectance. Intensity-dependent Bragg scattering is explained and distinguished from the effect of nonlinear absorption.

II. Experiments

A. Devices

The devices considered here, labeled sample A, optical element B, and optical element C, are shown in Fig. 1(a)–(c). The structures were grown on S-doped (001) InP 2-in single-side polished InP substrates; 10-nm protective InP layers were grown on top of all of the samples. Following the growth, multilayer antireflection coatings were deposited on the front surfaces of B and C, and the back sides of A, B, and C were polished to allow transmittance measurements without scattering . High sample quality and periodicity of the superlattice layers were confirmed by double crystal X-ray diffraction measurements.

A is made out of 121 10-nm $In_{0.530}Al_{0.141}Ga_{0.329}As$ barriers and 120 5-nm $In_{0.530}Ga_{0.47}As$ wells, resulting in a total thickness of the nonlinear sample of 1.81 μm.

B and C are both made out of two different sets of MQW each. In this work, a pair of adjacent MQW sets will be referred to as one *Bragg period*.

B is made out of MQW type 1 and MQW type 2, and has eight and a half Bragg periods. MQW type 1 consist of eight 10-nm $In_{0.530}Al_{0.141}Ga_{0.329}As$ barriers and seven 5-nm

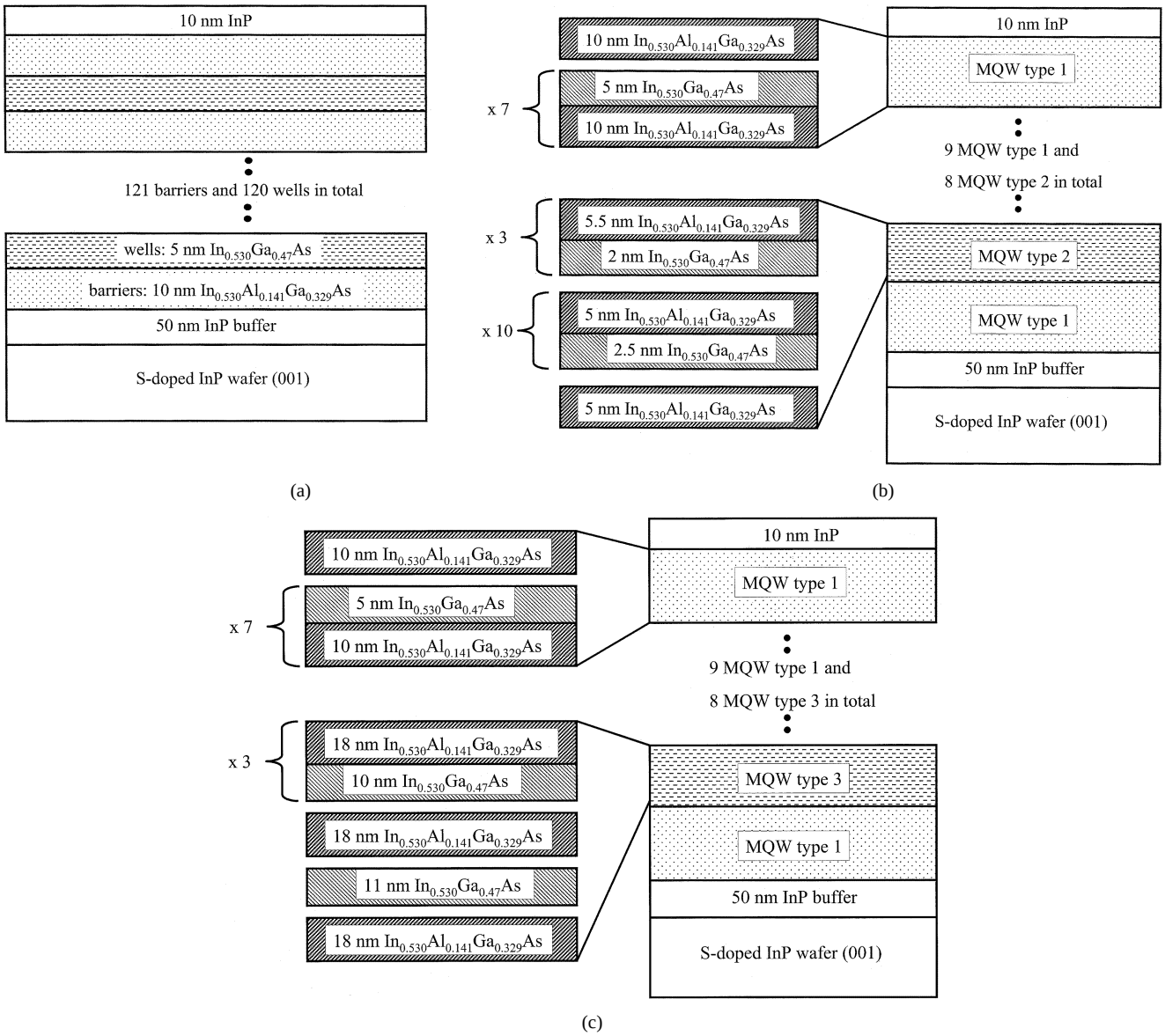

Fig. 1. Cross sections of the nonlinear samples analyzed: (a) a MQW sample A; (b) a double-MQW sample B; and (c) a double-MQW sample C.

$In_{0.530}Ga_{0.47}As$ wells. MQW type 2 is made out of three pairs of 5.5-nm $In_{0.530}Al_{0.141}Ga_{0.329}As$ and 2-nm $In_{0.530}Ga_{0.47}As$ grown on the top of 11 5-nm $In_{0.530}Al_{0.141}Ga_{0.329}As$ barriers interleaved with ten 2.5-nm $In_{0.530}Ga_{0.47}As$ quantum wells. The total thickness of B is 1.855 μm.

C has 8.5 MQW type-1/MQW type-3 Bragg periods. MQW type-3 consists of five 18-nm $In_{0.530}Al_{0.141}Ga_{0.329}As$ barrier layers separated from each other by three 10-nm $In_{0.530}Ga_{0.47}As$ and one 11-nm $In_{0.530}Ga_{0.47}As$ well, giving the total thickness of C of 2.083 μm.

It was sought to meet two criteria in designing B and C. The periodicity of B and C were chosen so that constituent pairs of MQW form a Bragg grating with spectral resonance in the vicinity of 1.5 μm in both optical elements. Moreover, in order to approximate matching of linear indices between the constituent MQW pairs in samples B and C, the average compositions of MQW type 1, type 2, and type 3 were chosen to be similar.

As a result of the similar average composition and Bragg periodicity, B and C contain hidden gratings whose reflectivity emerges via intensity-dependent changes in the effective refractive indices of the constituent MQW. This phenomenon, combined with the strong saturation of absorption, accounts for changes in reflectance and transmittance observed and reported in Section III.

B. Linear Optical Properties

The photoluminescence (PL) and linear transmittance spectra of A, B, and C, are shown in Figs. 2 and 3. Sample A has a PL peak and a strong excitonic feature in transmittance at 1517 nm, corresponding to the first allowed optical transition in the constituent MQW. The PL peak of B at 1493 nm is attributed to the lowest transition of MQW type 1. Since the first allowed transition in MQW type 2 is very weakly confined, there is no second PL peak. The PL spectrum of C shows two PL peaks and excitonic steps in transmittance: the lower wavelength feature at

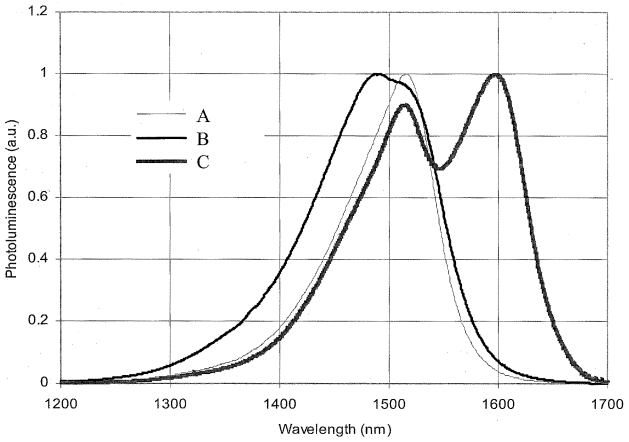

Fig. 2. Photoluminescence spectra of A, B, and C.

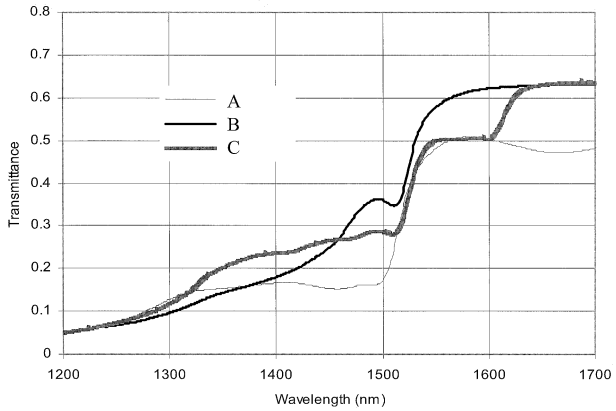

Fig. 3. Linear transmittance spectra of A, B, and C.

1517 nm due to MQW type 1 and the longer wavelength feature at 1600 nm, corresponding to the lowest transition of the second set of MQW type 3.

C. Nonlinear Optical Properties: Experimental Apparatus

The experimental apparatus used in nonlinear reflectance and transmittance measurements is shown in Fig. 4. The laser beam was focused using a 55-cm focal length lens onto samples placed perpendicular to the beam. The radius of the beam waist at the focus, measured at the $1/e^2$ of the transverse beam intensity profile, ranged from 91 μm at a wavelength of 1300 nm to 112 μm at 1600 nm. In order to monitor incident power, a portion of the incident beam was sampled using a wedged beamsplitter. This beamsplitter was also used to deflect a portion of the beam reflected from the sample. The power transmitted through the sample, as well as a fraction of the reflected power, was recorded as the incident power was varied. From this, the power-dependent transmittance and reflectance of each structure were obtained.

Nonlinear measurements were made using a picosecond laser amplification system which consists of four parts: light conversion topas optical parametric amplifier, quantronix titan Ti : sapphire amplifier, quantronix frequency-doubled Nd : YLF Q-switched pump laser, and coherent diode-pumped ultrafast laser vitesse seed source. This wavelength-tunable system works at a repetition rate of 1 kHz. Autocorrelation

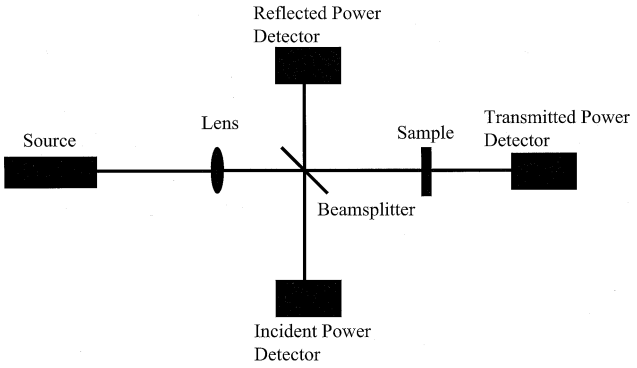

Fig. 4. Experimental setup used in the nonlinear transmittance and reflectance measurement.

measurements gave a pulsewidth (FWHM) of $\tau_p = 1.2$ ps. The signal and idler beams from the OPA were wavelength separated and the intensity of the signal beam used in the experiments was controlled using crossed polarizers with a half-waveplate inserted.

III. Results and Discussion

The nonlinear transmittance (T) and reflectance (R) of the three structures A, B, and C were measured in the wavelength range of 1300 to 1600 nm, at average incident powers ranging from 0.3 to 100 μW. This correspond to pulse energies between 300 pJ and 100 nJ and fluences ranging from 1 μJ/cm^2 to 320 μJ/cm^2. The results are shown in Figs. 5–8.

A. Nonlinear Response of A

Fig. 5(a) and (b) shows the change in the transmittance (defined as $T - T_{\text{initial}}$) and reflectance (defined as $R - R_{\text{initial}}$) of A. The insets show the intensity-dependent evolution of T and R at two representative wavelengths, 1420 and 1500 nm. At a given wavelength, as the incident fluence increases, the absorption of the sample saturates due to bandfilling. With decreasing absorption, T increases and the power reflected from the back side of the wafer rises, increasing total R. The time required for the free carriers excited by the laser pulse to relax back to the valence band is at least few hundreds of picoseconds, which is much longer than the round trip of the pulse in the sample $\sim$ps. As a result the contribution to R from back reflection off the wafer-air interface varies $\propto T^2$. The shapes of the transmittance and reflectance spectra of Fig. 5(a) and (b), respectively, follow the same trends, which suggests that the only contribution to the change in R is that from the change in back reflection at the wafer-air interface. The change in total R from the nonlinear reflectivity changes of the sample-air and sample-wafer interfaces are negligible.

The largest changes in T and R of sample A are observed around the excitonic peak of MQW type 1 in the vicinity of 1.5 μm. Here, the threshold for the saturation of absorption is lowest. With decreasing wavelength, the number of unoccupied carrier states needing to be saturated increases. As a consequence, the change in R and T is decreased for a fixed incident power. For wavelengths longer than that corresponding to the bandgap ($\lambda > 1520$ nm), there is small negative change in T

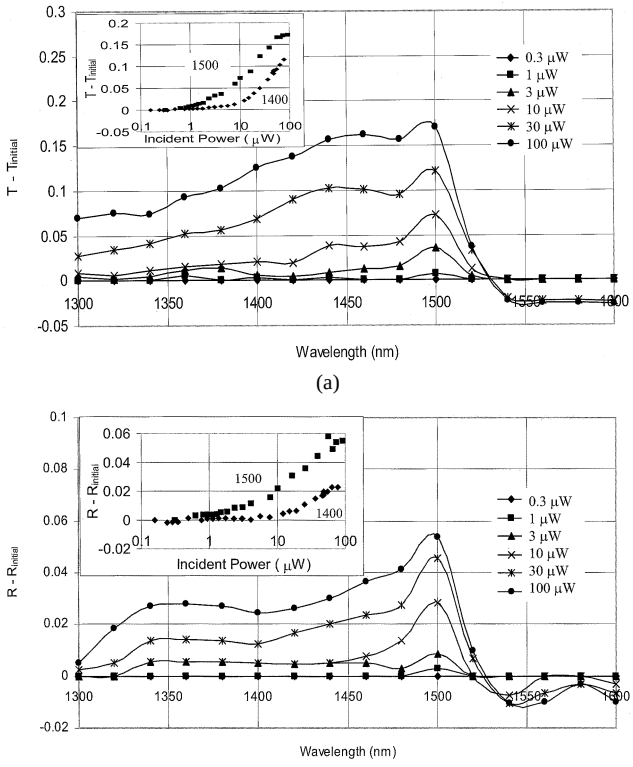

(a)

(b)

Fig. 5. Nonlinear response of MQW sample A. (a) Change in the absolute transmittance of A in the spectral range 1300 to 1600 nm, at incident powers of 0.3, 1, 3, 10, 30 , and 100 μW. (b) Change in absolute reflectance of sample A, under the same conditions as in (a).

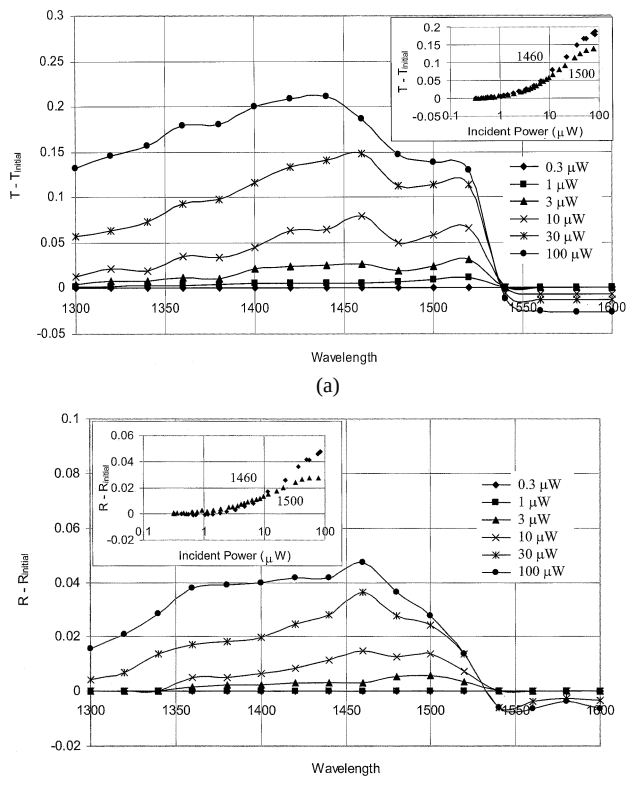

(a)

(b)

Fig. 6. Power-dependent change in the (a) transmittance and (b) reflectance of the double-MQW sample B under the same conditions as in Fig. 5.

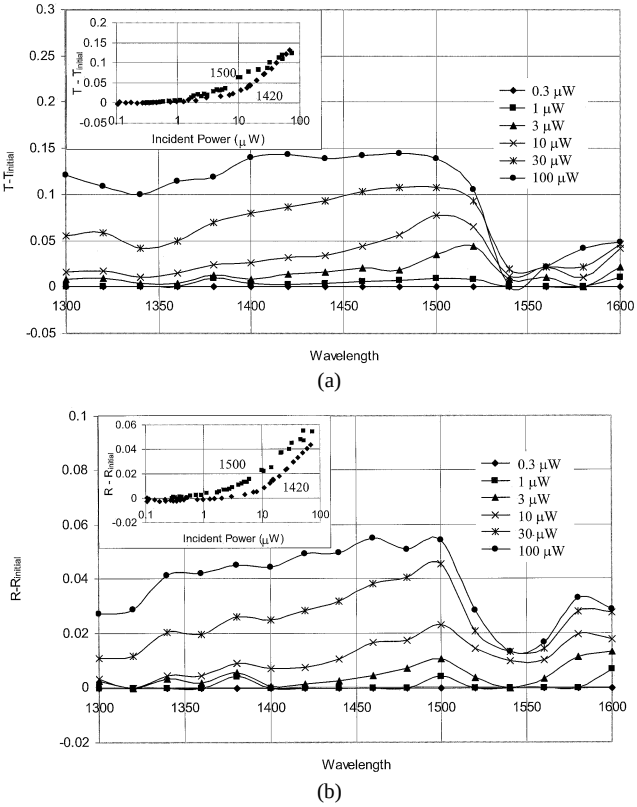

(a)

(b)

Fig. 7. Power-dependent change in the (a) transmittance and (b) reflectance response of the sample C under the same conditions as in Fig. 5.

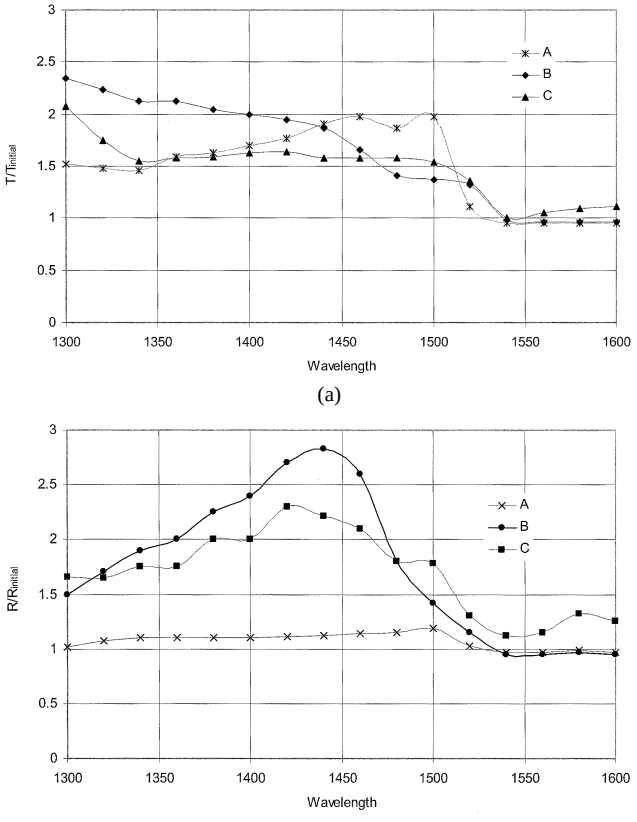

(a)

(b)

Fig. 8. Relative changes in (a) T and (b) R of the samples analyzed at incident power of 100 μW.

=m and R due to the two-photon absorption (2PA) in the InP substrate. 2PA is a much weaker nonlinear effect than saturation of resonant absorption in A and requires a higher *fluence* $\times$ *length* product to be observed. Near 1525 nm, the effect of the saturation of absorption in sample A and 2PA in the substrate cancel each other almost exactly. As a result, the change in T and R of A is negligible.

B. Nonlinear Response of B

The nonlinear reflectance and transmittance spectra of B are shown in Fig. 6(a) and (b). The nonlinear response of B in the absorbing region ($\lambda < 1540$ nm) is similar to that of A: T and R increase with increasing incident power. Thus, the major nonlinear effect in B is again saturation of absorption. However, at some spectral ranges, the corresponding $R - R_{\text{initial}}$ and $T - T_{\text{initial}}$ curves do not resemble each other as closely as in A. In fact, at some wavelength the responses of R and T show opposite trends.

At high incident powers, the change in T around the excitonic peak of 1.5 μm is diminished with respect to the change in T at other wavelengths above the bandgap. This behavior is opposite to that observed in A, where the change in T was most pronounced around the bandgap. The largest change in R of B is near 1500 nm at low incident powers and around 1460 nm at high incident powers. 1460 nm is a significantly lower wavelength than the absorption onset of MQW type 1 of B, which happens around 1520 nm. Also, in Fig. 6(a), for moderate powers (1 μW, 10 μW, 30 μW) there is a dip around 1480 nm, which becomes a plateau in the range 1480 to 1520 nm at 100 μW. This is again in contrast to the behavior seen in Fig. 6(b), where there is no dip around 1480 nm, and for powers of 30 and 100 μW, the change in R is very distinctly peaked at 1460 nm.

The differences in the nonlinear R and T response of B are attributed to the combination of saturation of the absorption and the power-dependent nonlinear coherent Bragg backscattering. B is made out of two sets of MQW whose linear indices are initially closely matched. As the intensity increases the absorption of MQW type 1 becomes saturated, at the same time changing its effective refractive index. A Bragg grating appears in the vicinity of 1.5 μm. This dynamic Bragg grating enhances R and diminishes T in the range 1480 to 1520 nm.

The insets of Fig. 6(a) and (b) show the change in R and T as function of the incident power for 1460 and 1500 nm. As is also evident from the spectral plot, the change in R at 1460 nm is initially lower than the change in R at 1500 nm, but then becomes higher for incident powers larger than 10 μW. In contrast, the change in T of B at 1460 nm is always higher than or equal to the change in T at 1500 nm.

Similar to the response seen in A for wavelengths longer than the lowest transition level of MQW type 1, 2PA of the InP substrate is the only measurable nonlinear effect. Again, near 1520 nm, the effect on nonlinear change in R and T of the saturation of absorption and 2PA cancel each other out.

C. Nonlinear Response of C

In Fig. 7(a) and (b), the nonlinear T and R response of C is shown. Saturation of absorption is again the dominant nonlinear effect. Similar to B, the R and T change curves show opposite trends in certain spectral regions.

The change in T is peaked near the exciton at 1500 nm for incident powers of 3 and 10 μW and then becomes increasingly flat in the range 1400–1500 nm. This is in contrast to the behavior in Fig. 7(b)—a change in R is peaked at 1500 nm for all incident powers. Such a response suggests a growing photonic stopband around 1500 nm. In C, both sets of MQW exhibit saturation of absorption and refractive nonlinearity. However, the expected nonlinear index change of MQW type 1 is much larger than that of MQW type 3, and hence a net index contrast emerges.

The insets in Fig. 7(a) and (b) confirm the different response of R and T. Whereas the change in T at 1500 nm is initially larger than or equal to the change in T at 1420 nm, the change in R at 1500 nm is always larger than the change of R at 1420 nm.

Since C absorbs beyond 1600 nm, 2PA from the wafer is not observable—the saturation of absorption dominates.

The differences in the nonlinear response of the three samples analyzed are further displayed in Fig. 8(a) and (b), where the relative changes in transmittance ($T_{\text{rel}} = T/T_{\text{initial}}$) and reflectance ($R_{\text{rel}} = R/R_{\text{initial}}$) of A, B, and C are shown. These results correspond to the maximum recorded changes, measured at 100 μW. The three samples show T_{rel} between 1.5 and 2 for the spectral region $\lambda < 1500$ nm. The T_{rel} of A is largest near the excitonic peak of 1500 nm. T_{rel} of B is diminished around 1500 nm, while T_{rel} of C is flat in the region 1350 nm $< \lambda <$ 1500 nm. The R_{rel} of B and C peaks around 1450 nm, while R_{rel} of A peaks again around 1500 nm. The large difference in the maximum R_{rel}, of A ($\sim$1.25) and R_{rel} of B and C ($\sim$2.8 and $\sim$2.3, respectively) is because only B and C have antireflection coatings and in effect have much lower initial reflectance.

D. Numerical Analysis

In this subsection, a simple numerical model is used to further explain the results reported above. The nonlinear steady-state transfer matrix model discussed in detail in [19] has been extended to account for the absorption, saturation of absorption, and saturation of the nonlinear index change. The complex effective index of refraction of an mth layer was assumed to exhibit power dependence according to

$$n_m = n_{0m} + \frac{n_{2m}P}{1 + \frac{P}{P_{\text{satm}}}} + i\frac{\kappa_{0m}}{1 + \frac{P}{P_{\text{samt}}}} \tag{1}$$

where n_{0m} is the linear refractive index, n_{2m} is the nonlinear coefficient, κ_{0m} is related to the linear absorption by $\kappa_{0m} = \alpha_{0m}\lambda/4\pi$, P is local average power, and P_{satm} is the saturation power. The n_2 used in (1) is not an ultrafast Kerr coefficient (expressed in units of inverse intensity), but a nonlinear coefficient that has units of inverse power. Resonant nonlinearities give rise to index changes proportional to power (or fluence) rather than to the instantaneous peak intensity.

The results of the simulations are shown in Fig. 9. The change in the transmittance and reflectance with increasing incident power was computed for two structures illuminated with light at a wavelength of 1.5 μm. Fig. 9(a) shows the response of the

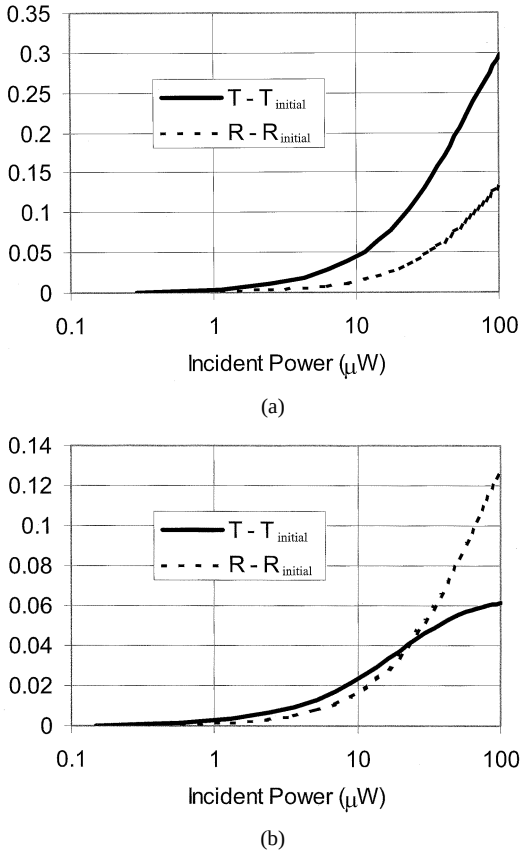

Fig. 9. Simulated results of a change in the absolute transmittance and reflectance of (a) a sample of uniform nonlinear absorbing material and (b) a sample with a pop-up Bragg grating.

structure made out of eight and a half Bragg periods of a homogeneous material—a sample that will never exhibit Bragg resonance. The nonlinear response of this sample is analogous to that observed in A. In agreement with previous measurements with the same laser source [18], the coefficients of the constituent material were taken to be $\alpha_0 = 6000$ cm^{-1} and $n_2 = 6 \times 10^{-9}$ W^{-1}. This gave the maximum induced nonlinear index change of $\Delta n = 0.14$ [18]. According to the ellipsometric measurements, the linear index of refraction of the constituent MQW is $n_0 = 3.47$. Saturation power was estimated to be 100 μW. A constant reflection at the back facet-air interface of $R_{\text{back-airr}} = 0.28$ was assumed, while the front facet of the simulated samples was taken to be anti-reflection coated.

As observed in Fig. 5 in the response A, the intensity-dependent changes in R and T shown in Fig. 9(a) are of a similar shape. With the increasing intensity, the absorption saturates. Since no nonlinear Bragg scattering is present, both T and R increase monotonically.

Fig. 9(b) shows the nonlinear response of the structure analogous to B and C in the spectral ranges 1480–1520 nm (sample B) and around 1500 nm (sample C). The structure analyzed is assumed to be made out of eight and a half Bragg periods, where one of the constituent materials has properties like the material in Fig. 9(a), while the other material is nonabsorbing and linear ($\alpha_0 = 0$ and $n_2 = 0$). The materials are assumed to have matched linear indices ($n_{01} = n_{02} = 3.47$). Again, the dominant feature in the simulated nonlinear response is the saturation of the absorption which results in the initially monotonically increasing R and T. However, for higher incident power, the effect of the growing Bragg grating becomes evident: as the reflectance continues to increase, the transmittance saturates.

IV. Conclusions

Measurements of nonlinear transmittance and reflectance of three semiconductor one-dimensional structures were reported. The first MQW sample showed strong saturation of absorption, which was most visible around the excitonic peak. Two of the analyzed structures have a built-in periodicity which gives rise to a power-dependent Bragg grating with resonance near 1.5 μm. The nonlinear response of these two Bragg periodic samples is influenced by both nonlinear absorption and nonlinear contradirectional coupling. The effect of the nonlinear pop-up grating and the effect of the saturation of the absorption were distinguished by comparison of the behavior of Bragg-periodic superlattices with that of a pure MQW.

The strong nonlinear response of the analyzed structures observed over a broad spectral range of 1.3–1.6 μm suggests their potential applicability as optical devices. We did not measure the relaxation time of our samples, expected to correspond to a typical exciton recombination time in direct-bandgap semiconductors of a few nanoseconds. Rapid recovery would be enabled by established techniques of low-temperature growth resulting in reduction of the relaxation time down to the tens of picosecond range [20], [21].

References

[1] G. I. Stegeman, "Material figures of merit and implications to all-optical waveguide switching," in *Nonlinear Optical Properties of Advanced Materials, SPIE 1882*, 1993, pp. 75–89.
[2] P. W. E. Smith and L. Qian, "Switching to optical for a faster tomorrow," *IEEE Circuits Devices Mag.*, vol. 15, pp. 28–33, 1999.
[3] L. Brzozowski and E. H. Sargent, "Optical signal processing using nonlinear distributed feedback structures," *IEEE J. Quantum Electron.*, vol. 36, pp. 550–555, 2000.
[4] J. He and M. Cada, "Optical bistability in semiconductor periodic structures," *IEEE J. Quantum Electron.*, vol. 27, pp. 1182–1188, 1991.
[5] N. G. R. Broderick, D. Taverner, D. J. Richardson, M. Ibsen, and R. I. Laming, "Optical pulse compression in fiber Bragg Gratings," *Phys. Rev. Lett.*, vol. 79, pp. 4566–4569, 1997.
[6] W. N. Ye, L. Brzozowski, E. H. Sargent, and D. Pelinovsky, "Stable all-optical limiting in nonlinear periodic structures III: Non-solitonic pulse propagation," J. Opt. Soc. Amer. B, vol. 20, no. 4, pp. 695–705, 2003, to be published.
[7] N. G. R. Broderick, D. Taverner, D. J. Richardson, M. Ibsen, and R. I. Laming, "Experimental observation of nonlinear pulse compression in nonuniform Bragg gratings," *Opt. Lett.*, vol. 22, pp. 1837–1839, 1997.
[8] C. J. Herbert, W. S. Capinski, and M. S. Malcuit, "Optical power limiting with nonlinear periodic structures," *Opt. Lett.*, vol. 17, pp. 1037–1039, 1992.
[9] D. Pelinovsky, L. Brzozowski, J. Sears, and E. H. Sargent, "Stable all-optical limiting in nonlinear periodic structures," *J. Opt. Soc. Amer. B*, vol. 19, pp. 43–53, 2002.
[10] L. Brzozowski and E. H. Sargent, "All-optical analog-to-digital converters, hard limiters, and logic gates," *J. Lightwave Technol.*, vol. 19, pp. 114–119, 2001.
[11] J. E. Sipe and H. G. Winful, "Nonlinear Schroedinger solitons in a periodic structure," *Opt. Lett.*, vol. 13, pp. 132–133, 1998.
[12] D. L. Mills and S. E. Trullinger, "Gap solitons in nonlinear periodic structures," *Phys. Rev. B*, vol. 36, pp. 947–952, 1987.
[13] G. Pan, R. Kesavamoorthy, and S. A. Asher, "Optically nonlinear Bragg diffracting nanosecond optical switches," *Phys. Rev. Lett.*, vol. 78, pp. 3860–3863, 1997.

[14] Y. Lin, J. Zhang, E. H. Sargent, and E. Kumacheva, "Photonic pseudo-gap-based modification of photoluminescence from CdS nanocrystal satellites around polymer microspheres in a photonic crystal," *Appl. Phys. Lett.*, vol. 81, pp. 3134–3136, 2002.
[15] J. Carroll, J. Whiteaway, and K. Plumb, *Distributed Feedback Semiconductor Lasers*. Bellingham, WA: SPIE, 1998.
[16] M. Kawase, E. Garmire, H. C. Lee, and P. D. Dapkus, "Single-pulse pump-probe measurements of optical nonlinear properties in GaAs/AlGaAs multiple quantum wells," *IEEE J. Quantum Electron.*, vol. 30, pp. 981–988, 1994.
[17] S. H. Park, J. F. Morhange, A. D. Jeffery, R. A. Morgan, A. Chavez-Pirson, H. M. Gibbs, S. W. Koch, N. Peyghambarian, M. Derstine, A. C. Gossard, J. H. English, and W. Weigmann, "Measurement of room-temperature -gap-resonant optical nonlinearities of GaAs/AlGaAs multiple quantum wells and bulk GaAs," *Appl. Phys. Lett.*, vol. 52, pp. 1201–1203, 1988.
[18] L. Brzozowski, E. H. Sargent, A. SpringThorpe, and M. Extavour, "Direct measurements of large near-bandedge nonlinear index change from 1.48–1.55μm in InGaAs/InAlGaAs multi-quantum-wells," Appl. Phys. Lett., submitted for publication.
[19] L. Brzozowski and E. H. Sargent, "Nonlinear distributed feedback structures as passive optical limiter," *J. Opt. Soc. Amer. B*, vol. 17, pp. 1360–1365, 2000.
[20] H. S. Loka, S. D. Benjamin, and P. W. E. Smith, "Optical characterization of GaAs for ultrafast switching devices," *IEEE J. Quantum Electron.*, vol. 34, pp. 1426–1437, 1998.
[21] L. Qian, S. D. Benjamin, P. W. E. Smith, B. J. Robinson, and D. A. Thompson, "Picosecond carrier lifetime and large optical nonlinearities in InGaAsP grown by helium-plasma-assisted molecular beam epitaxy," *Opt. Lett.*, vol. 22, no. 108, pp. 108–110, 1997.

Lukasz Brzozowski received the B.Sc. (Hons.) degree with high distinction from the University of Toronto, Toronto, ON, Canada, in 1999, with a specialization in physics and mathematical sciences. He is currently working toward the Ph.D. degree in the Photonics Group, Department of Electrical and Computer Engineering, University of Toronto.

During the summer of 2000, he was a Visiting Scientist at the Laboratoire Photonique Quantique et Moldculaire, Ecole Normale Supdrieure de Cachan, Paris, France. He holds a postgraduate Scholarship from Canada's National Sciences and Engineering Research Council. His research interests include linear and nonlinear characterization of organic, semiconductor, and nanocrystal material systems, and fabrication and design of nonlinear switching devices.

Vlad Sukhovatkin received the M.Sc. degree in physics from Kiev State University, Kiev, Ukraine, in 1986.

He was with the Institute of Physics, Kiev, Ukraine, and the engineering company Dynamic Ltd., conducting research in the field of nonlinear optics and ultrafast laser systems. In 2002, he joined the Photonics Group, University of Toronto, Toronto, ON, Canada, as a Research Engineer.

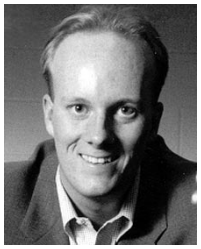

Edward (Ted) H. Sargent holds the Nortel Junior Chair in Emerging Technologies in the Department of Electrical and Computer Engineering and also the Nortel Networks—Canada Research Chair in Emerging Technologies, both at the University of Toronto, Toronto, ON, Canada. He leads a group of 12 graduate and post-doctoral researchers in the areas of semiconductor quantum electronic devices, photonic crystal applications, hybrid organic inorganic quantum-dot electroluminescence, and multiple-access optical networks.

In 1999, Dr. Sargent was awarded both the Silver Medal of the Natural Sciences and Engineering Research Council of Canada for his work on the lateral current injection laser and the Premier's Research Excellence Award in recognition of research into the application of photonic crystals in lightwave systems. In 2001, the Canada Research Chairs Foundation wrote that Ted Sargent has "… shown that a new kind of photonic macrocrystal—one which harnesses nature's underlying drive toward symmetry—will transform how communication networks are built." In 2002, the Canadian Institute for Advanced Research named him one of the nation's top 20 researchers under age 40 across the natural sciences, engineering, and social sciences. In 2002, he won the IEEE Canada Outstanding Engineer Award for "for groundbreaking research in applying new phenomena and materials from nanotechnology toward transforming fiber-optic communications systems into agile optical networks." His contributions have led to well over 100 contributed and invited papers in refereed journals, conference proceedings, and institutional lectures in IEEE, Optical Society of America, American Institute of Physics, and Materials Research Society publications and conferences. He has chaired conferences and symposia, including thee Photonic Networks Symposium at IEEE Globecom and the first Canada-France Conference on Molecular Photonics and Plastic Electronics.

Anthony (Tony) J. SpringThorpe received the B.Sc. degree in physics in 1963 and the Ph.D. degree in solid-state physics in 1967, both from the University of Sheffield, Sheffield, U.K.

During 1967–1969, he held a post-doctoral Fellowship at the University of Bath, Bath, U.K., investigating many of the ternary analogs of III–V compound semiconductors (such as $ZnSiP_2$), which resulted in the first preparation of two new compounds: $MgSiP_2$ and SiP_2. In October 1969, he joined Northern Electric R&D Labs, later to become Bell-Northern Research, and now Nortel Networks, Nepean, ON, Canada. As a Member of Scientific Staff, he was responsible for liquid-phase epitaxial growth techniques for the preparation of III–V compound semiconductors—initially for visible light-emitting diodes, but subsequently for near infra-red lasers in the GaAs–AlGaAs and GaInAsP alloy systems. During the next ten years, this work led to the development of processes for the preparation and fabrication of a wide range of optoelectronic devices, many of which saw application in the first generation of fiber optic transmission systems. Recognizing the potential of metal organic chemical vapor deposition (MOCVD) for the controlled deposition of III–V compound semiconductors on large-area substrates, he designed and built the first Canadian MOCVD system in 1978. Building on this experience, in the mid 1980s, he was instrumental in introducing MOCVD and molecular beam epitaxy (MBE) to Nortel for the production of the next generation of III–V compound device structures. Many of the devices developed during this period formed the foundation of Nortels' success in the fiber optic field. He was the Manager of Epitaxy, Nepean, Canada, from 1978 to 1997, and a New Materials Advisor in the High Performance Optical Components Division of Nortel Networks until May 2002. Since then, he has joined the National Research Council of Canada as a Principal Research Officer in the Institute of Microstructural Sciences, continuing research work on III–V compound material epitaxy. He currently holds numerous patents on various aspects of III–V compound semiconductor epitaxy and devices, and during his professional life has contributed to many publications and presentations on materials and devices.

In 1977, Dr. Springthorpe was awarded the W. Lash Miller Prize of the Electrochemical Society for his work on the development of III–V compound materials and devices. In 1997, he was awarded the Nortel Presidents' Prize for technology cascade, in recognition of his long-term contribution to the success of the Nortel optoelectronics program. Most recently, he was the winner of the MANTECH2002 "Ugly photo" competition.

Marcius Extavour currently working toward the B.S. degree physics in the Engineering Science Program at the University of Toronto, Toronto, ON, Canada. His thesis research explores carrier dynamics in luminescent nanocrystal/polymer composites.

During 2001–2002, he worked with Dr. SpringThorpe on the epitaxial growth and characterization of III–V heterstructures at Nortel Networks Corporation, Ottawa, ON, Canada.